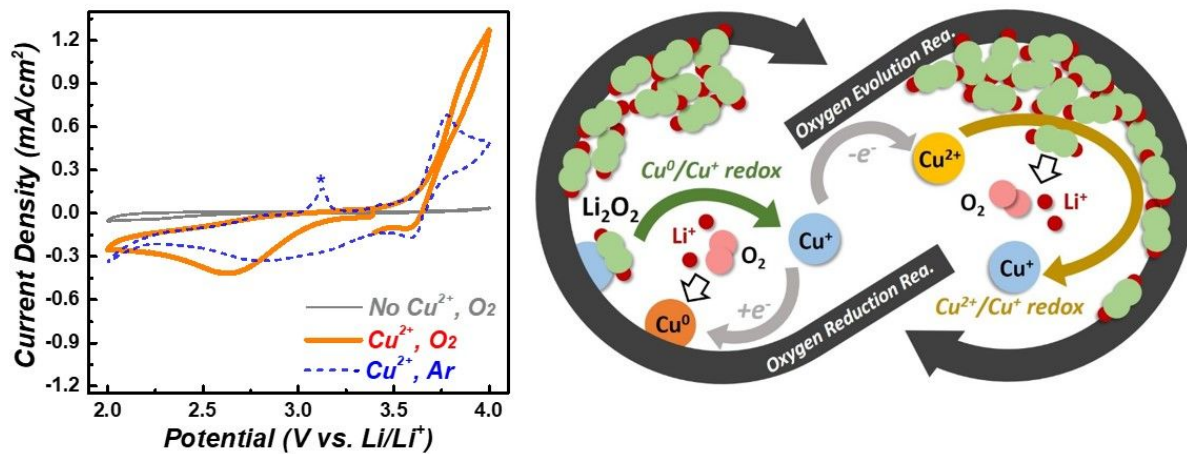




Two birds with one stone: Cu ion redox mediation for non-aqueous Li-O₂ battery

Journal:	<i>Journal of Materials Chemistry A</i>
Manuscript ID	TA-COM-05-2019-004946.R1
Article Type:	Communication
Date Submitted by the Author:	17-Jun-2019
Complete List of Authors:	Deng, Han; AIST, Qiao, Yu; National Institute of Advanced Industrial Science and Technology (AIST), Zhang, Xueping; Nanjing University, School of Electronic Science and Engineering Qiu, Qeilong; Nanjing University Chang, Zhi; AIST, He, Ping; Nanjing University, College of Engineering and Applied Sciences; National Institute of Advanced Industrial Science and Technology, Energy Technology Research Institute Zhou, HaoShen; AIST, ; Nanjing university, Center of Energy Storage Materials & Technology



A simple metal ion additive has been employed as a multi-functional redox mediator for Li-O₂ battery.

COMMUNICATION

Two birds with one stone: Cu ion redox mediation for non-aqueous Li-O₂ battery

Received 00th January 20xx,
Accepted 00th January 20xx

Han Deng,^{abc} Yu Qiao,^{*b} Xueping Zhang,^a Feilong Qiu,^a Zhi Chang,^{bc} Ping He^a and Haoshen Zhou^{*}
^{abc}

DOI: 10.1039/x0xx00000x

The aprotic Li-O₂ battery is considered as a promising high energy storage system, though its practical application is stumbled by the high overpotential and parasitic reaction. Herein, it's shown that by the addition of soluble Cu ion, the Li₂O₂ electrochemistry on both discharge and charge processes can be mediated by different redox couples of Cu ion. The improved capacity is achieved by a Cu⁺/Cu⁰ redox mediated reaction pathway and the 3.6 V Cu⁺/Cu²⁺ redox couple helps reduce the charge overpotential. Meanwhile, benefitting from suppression of reactive superoxide intermediate and a mild charge potential, the parasitic reaction is effectively inhibited. Not rigidly limited within the organic compound candidates, the introduction of the inorganic Cu ion, as a multi-functional mobile additive, would open up a new gate for the design of the metal ion redox mediators for Li-O₂ batteries.

Owing to its extremely high theoretic energy density, the lithium oxygen (Li-O₂) battery is considered as a promising candidate for the post Li-ion battery systems.^[1-2] The working principle of a typical aprotic Li-O₂ battery is based on the reversible formation/decomposition of Li₂O₂ on a carbon cathode during oxygen reduction reaction (ORR) and oxygen evolution reaction (OER). Unfortunately, there are plenty of challenges that should be addressed before the practical application of Li-O₂ battery.^[3-5] During ORR, the sluggish charge transfer through the insulating Li₂O₂ will lead to the early cell death.^[6-7] And the heterogeneous solid/solid (electrode/Li₂O₂) contact mode results in high overpotential in the OER, giving rise to cell component degradation and poor energy efficiency.^[4]

Moreover, the superoxo-derived parasitic reaction threatens the stability and reversibility of the Li-O₂ electrochemistry.^[5]

Though solid catalysts have been designed for improving the capacity and lowering the overpotential of Li-O₂ battery, the catalysis through the solid/solid interface is still considered not essential to solve the kinetic concern.^[8-10] By alternating the reaction process into a solution pathway, redox mediators (RMs) can provide a new catalytic mode in a homogeneous way, which is recently considered as an effective method to restrain the above mentioned inherent defects.^[11-12] In order to solve the corresponding problems during ORR and OER, RMs can be cataloged into two types, namely RM_R and RM_E. During ORR, prior to the O₂ reduction, RM_R is reduced into RM_R⁻ at the cathode. Then RM_R⁻ transfers the electron to the O₂ to form Li₂O₂, boosting the Li₂O₂ deposition via a solution-mediated pathway.^[13-15] During OER, the RM_E⁺ oxidized firstly at the cathode side uniformly spreads to the Li₂O₂ deposits and chemically decomposes them into O₂, while itself reverts to the pristine RM_E state. With the OER potential determined by the RM_E/RM_E⁺ redox couple, the charge overpotential can be effectively controlled.^[16-18] Combining them together, the dual mediator strategy can simultaneously and synchronously achieve a higher reversible capacity with an increased energy efficiency.^[19-21] However, employing multiple additives to the electrolyte inevitably aggravates the complexity of the battery system. Thus, researchers are urgently eager for an individual additive that can address multiple problems. Zhang et al. fabricated different functional radicals on the electrolyte molecular to enhance both ORR and OER process through a solution-mediated way for Li-O₂ batteries. So far, there are still very few reports on multi-functional RMs towards ORR and OER.^[22-24] Moreover, overwhelming majority of research efforts focus on the organic compounds as potential candidates, while abundant inorganic candidates have been ignored.

In this work, by rationally utilizing the dual redox couples from a single additive, we introduce Cu ion to perform the ORR and OER missions simultaneously in the Li-O₂ battery. Working as a RM_R, the Cu⁺/Cu redox facilitates the Li₂O₂ formation, in the

^a Center of Energy Storage Materials & Technology, College of Engineering and Applied Sciences, Jiangsu Key Laboratory of Artificial Functional Materials, National Laboratory of Solid State Microstructures, and Collaborative Innovation Center of Advanced Microstructures, Nanjing University, Nanjing 210093, P. R. China. E-mail: kyou.qiaoyu09206@aist.go.jp; hszhou@nju.edu.cn

^b Energy Technology Research Institute, National Institute of Advanced Industrial Science and Technology (AIST), 1-1-1, Umezono, Tsukuba 305-8568, Japan

^c Graduate School of System and Information Engineering, University of Tsukuba, 1-1-1, Tennoudai, Tsukuba 305-8573, Japan

Electronic Supplementary Information (ESI) available: [details of any supplementary information available should be included here]. See DOI: 10.1039/x0xx00000x

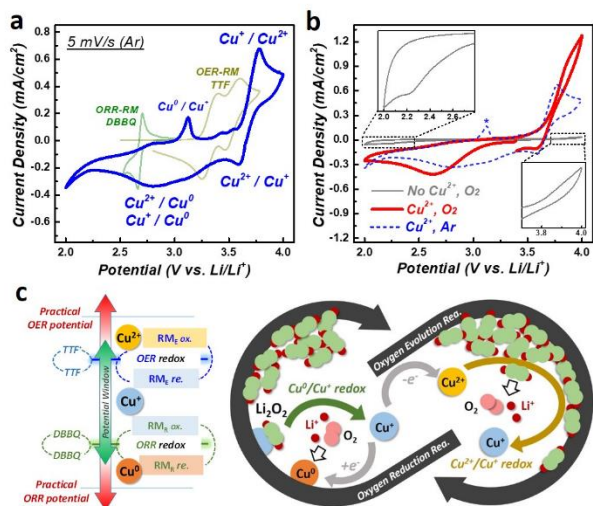


Fig. 1 a) Cyclic voltammetry (CV) curves in 1M LiTFSI-TEGDME electrolyte with the 50 mM Cu^{2+} ion RM additive under Ar atmosphere at a scan rate of 5 mV/s. CV curves of TTF and DBBQ are presented for comparison. b) CV curves in 1M LiTFSI-TEGDME electrolyte with or without the 50 mM Cu^{2+} ion RM additive under O_2 atmosphere at a scan rate of 5 mV/s. c) Schematic illustration of the proposed redox mediation mechanisms for Cu ion in $\text{Li}-\text{O}_2$ batteries.

meanwhile the $\text{Cu}^+/\text{Cu}^{2+}$ redox effectively mediates the decomposition of Li_2O_2 at a low potential as the RM_E . Moreover, by altering the reaction through the solution-mediated pathway, the Cu ion restrains the superoxo-derived parasitic reactions.

Since the redox potential is the essential parameter to assess the RM, the redox property of the Cu ion in aprotic electrolyte is firstly measured by cyclic voltammetry (CV) under inert Ar atmosphere (Fig. 1a). Two redox couples are clearly observed. The lower cathodic peak (~ 2.8 V vs. Li^+/Li , Cu^+/Cu^0) and higher anodic peak (~ 3.6 V vs. Li^+/Li , $\text{Cu}^+/\text{Cu}^{2+}$) are respectively located at the opposite sides of the theoretical thermodynamic potential (2.96 V vs. Li^+/Li) for the $\text{O}_2/\text{Li}_2\text{O}_2$, which exemplifies the feasibility of the Cu ion dual redox couples to act as both RM_R and RM_E . As classic RMs, the CV profiles of the 2,5-di-tert-butyl-1,4-benzoquinone (DBBQ, RM_R) and tetrathiafulvalene (TTF, RM_E) are shown for comparison.^[13, 18] Under O_2 atmosphere (Fig. 1b), the cathodic peak intensity with the Cu ion is largely prompted, and the peak position also exhibits an obvious positive shift from 2.2 V to 2.6 V vs. Li^+/Li compared to the Cu ion absent condition. From a kinetic aspect, this indicates the ORR process has been efficiently enhanced by the addition of Cu ion. After transferring the electron to O_2 , Cu^0 quickly reverts to Cu^+ , which can also be proved by the absence of Cu^0/Cu^+ oxidation peak during the anodic sweeping and the qualitative color reaction as identification of Cu^+ presence (Fig. S2). Moreover, compared to the Ar condition, the anodic $\text{Cu}^+/\text{Cu}^{2+}$ peak intensity has been largely enhanced under O_2 atmosphere, which indicates the mediation effect of the $\text{Cu}^+/\text{Cu}^{2+}$ redox couple for the chemical decomposition of Li_2O_2 . Meanwhile, the anodic peak at 3.6 V vs. Li^+/Li is much lower than the one observed in Cu ion absent condition.

Subsequently, based on the CV behavior, we propose the working mechanism of Cu ion additive as an effective RM towards both ORR and OER with $\text{Li}-\text{O}_2$ electrochemistry (Fig. 1c).

As revealed in Fig. 1b, the Cu ion redox couples exhibit competency for the RM working principles: (1) Similar as DBBQ, the reduction potential of Cu^+/Cu^0 redox is higher than the practical working potential during the discharge process. (2) Similar as TTF, the oxidation potential of $\text{Cu}^+/\text{Cu}^{2+}$ is lower than the practical decomposition potential for Li_2O_2 .^[22] Specifically, during the initial discharge process, the Cu^{2+} is firstly reduced at the cathode to Cu^+ , and then further reduced to the reductive state of RM_R , Cu^0 . While the presence of Cu^0 , it quickly interacts with the surrounding O_2 and Li^+ , transfers electron to form Li_2O_2 , and turns back to Cu^+ . During OER, Cu^+ is firstly oxidized to Cu^{2+} at the cathode. As the oxidative state of RM_E , Cu^{2+} facilitates the oxidation of Li_2O_2 particles, and reverts to Cu^+ . After effectively sweeping away the deposited Li_2O_2 from the cathode, a reversible process can be achieved.

Having confirmed the working principle of Cu ion as a RM, we investigate the $\text{Li}-\text{O}_2$ cell through the galvanostatic mode. During the discharge process, compared to the bare electrolyte condition, the ORR capacity is significantly improved on both carbon fiber cathode and porous KB cathode (Fig. 2a). The carbon fiber is a binder-free carbon-based cathode, consisted of fibers with a diameter of several micrometers (Fig. S1). It's a widely used cathode when studying the RM_R for $\text{Li}-\text{O}_2$ batteries.^[13, 15] With Cu ion in the electrolyte, a greatly improved areal capacity of ~ 0.40 mAh $\cdot\text{cm}^{-2}$ is observed compared with that (~ 0.13 mAh $\cdot\text{cm}^{-2}$) in the bare electrolyte. Note that the capacity of the Cu ion itself under Ar atmosphere is relatively low. This indicates the extended ORR capacity can be rationally ascribed to the Li_2O_2 formation. The corresponding dQ/dV result also proves the reduction of Cu ion prior to the oxygen reduction, which is well consistent with the CV results and the proposed working mechanism. Turing to a more

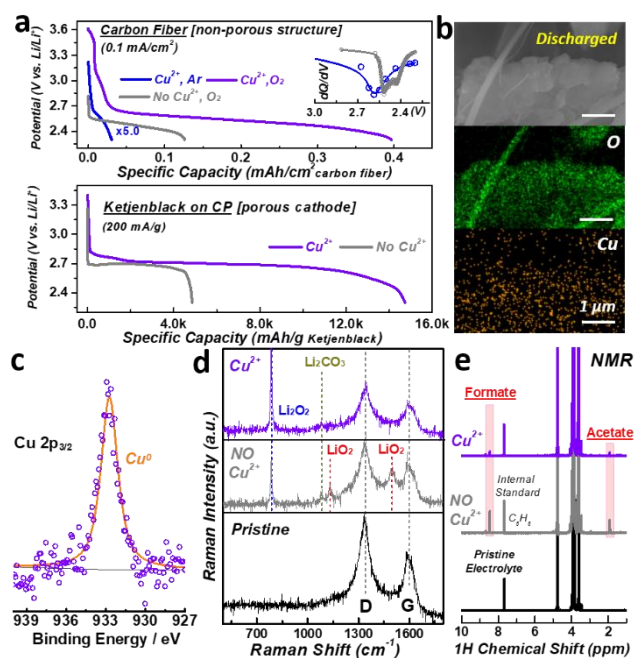


Fig. 2 a) Discharge profiles of $\text{Li}-\text{O}_2$ cells with and without Cu ion RM at different cathodes. b) SEM images, EDX mapping and c) $\text{Cu } 2p_{3/2}$ XPS spectrum of the discharged cathode. d) Raman spectra and e) ^1H NMR of the discharged cathodes with and without Cu ion RM. Both cathode and electrolyte in the separator are used for ^1H NMR.

practical porous KB cathode, the cell contained Cu ion RM delivers a specific capacity of $\sim 14700 \text{ mAh}\cdot\text{g}^{-1}$, equaling to $\sim 5.5 \text{ mAh}\cdot\text{cm}^{-2}$. This is a considerable areal capacity for Li-O₂ battery, which is also much improved compared with the bare electrolyte Li-O₂ cell. It's worth noting that the anion of the Cu salt we choose, Cl⁻, is reported to enhance the discharge capacity by incorporating into the discharge product to improve its electric conductivity.^[25] Nevertheless, the enhancement with solely Cl⁻ is quite limited (Fig. S3). We thus consider the increased capacity is dominated by the Cu⁺/Cu⁰ redox couple.

The SEM image and corresponding EDX mapping results are collected from the discharged cathode (2.3 V cut-off voltage, Fig. 2b). Besides the O element which is assigned to the discharge product Li₂O₂, Cu element can also be observed on the cathode at the end of discharge. Moreover, as revealed in the obtained Cu 2p_{3/2} XPS spectrum, a single peak at $\sim 932.7 \text{ eV}$ indicates the elemental state of the Cu, Cu⁰.^[26] Basically, due to the sluggish transport of the activity substances (O₂) at the end of discharge, the reductive state RM_R⁻ will definitely accumulate. Here, the presence of Cu⁰ on the cathode again proves the proposed mediation mechanism of the Cu⁺/Cu⁰ redox during ORR. Moreover, distinguished from other soluble RM_R, the reductive state RM_R⁻ (Cu⁰) for Cu⁺/Cu⁰ redox is a solid state anchored onto the cathode after discharge. The advantages of immobile RMs have received increasing concentration recently.^[27] The product information is further collected by Raman spectroscopy (Fig. 2d). Regardless of the D/G band from the pristine carbon cathode, the Li₂O₂ related peak (790 cm^{-1}) can be observed in both Cu ion contained and bare conditions, which is in accordance with the XPS results that Li₂O₂ is present as the discharge product (Fig. S4). More importantly, by the addition of Cu ion RM, the presence of the LiO₂ intermediate (peaks at 1135 and 1496 cm^{-1}) is greatly restrained, which indicates the Cu⁺/Cu⁰ redox mediation effect essentially alternates the original superoxo-related ORR pathway. Meanwhile, the parasitic production of Li₂CO₃ (1080 cm^{-1} , Raman peak) and carboxylates (1H NMR peak, Fig. 2e) has been simultaneously inhibited, in accordance with the FT-IR results (Fig. S6).^[28-29] Generally speaking, based on the Cu⁺/Cu⁰ redox couple, the solution-mediated ORR pathway has effectively enhance the discharge capacity, and the superoxo-derived parasitic reactions are also greatly inhibited.

During the charge process, a flat charge plateau at $\sim 3.5 \text{ V}$ is obtained with the addition of Cu ion under either a fixed capacity mode (Fig. 3a) or a voltage cut-off mode (Fig. S7), which is obviously different from the severely polarized overpotential observed in the bare electrolyte condition. The charge potential matches well with the CV results (Fig. 1a and 1b), indicating the function of Cu⁺/Cu²⁺ redox couple in the OER process. XRD results and corresponding SEM images primarily demonstrate the reversible formation/decomposition of Li₂O₂ particles during discharge and recharge in the Cu ion contained condition (Fig. 3b). More rigorously, gas evolution (O₂/CO₂) information has been collected by differential electrochemical mass spectrometry (DEMS, Fig. 3c). For the cell in bare electrolyte condition, the collected oxygen is observed with an obvious deviation from $2\text{e}^-/\text{O}_2$ process, accompanied with a serious release of CO₂. As a sharp comparison, the O₂ evolution keeps

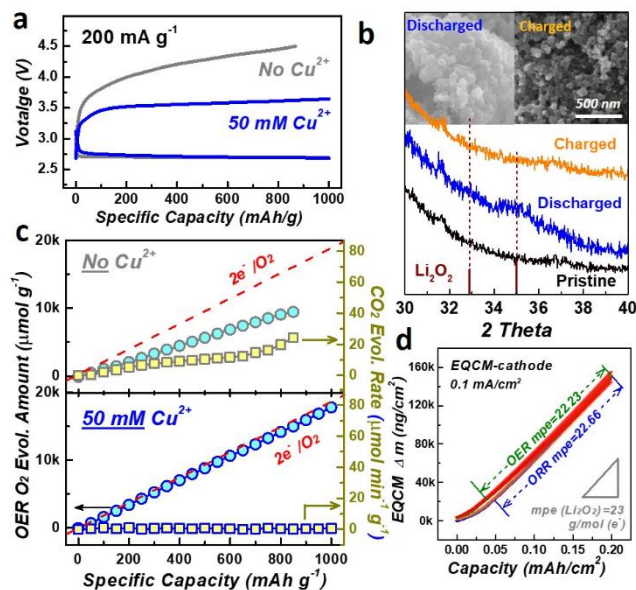


Fig. 3 a) Charge profiles of the Li-O₂ cells with and without Cu ion RM at $200 \text{ mA}\cdot\text{g}^{-1}$ and $1000 \text{ mA}\cdot\text{g}^{-1}$. b) SEM images and XRD spectrum of the discharged and charged cathodes in Li-O₂ batteries. c) O₂ evolution amount and CO₂ evolution rate during OER of Li-O₂ cells with and without Cu ion RM. d) Plots of mass change versus capacity during ORR and OER.

well with the pure Li₂O₂ decomposition ($2\text{e}^-/\text{O}_2$) process, and the parasitic CO₂ evolution can hardly be detected. These results demonstrate the Cu⁺/Cu²⁺ redox couple effectively suppressed the side reactions by controlling the charge potential within a mild range, thus improving the reversibility of Li₂O₂-based electrochemistry. Furthermore, corresponding quantitative information of the deposited products have also been revealed by the electrochemical quartz crystal microbalance (EQCM) analysis (Fig. 3d). Through the cathode mass variation rate (defined as mass change per electron, mpe), the EQCM results corroborate that the reversible Li₂O₂ deposition/decomposition process dominates most of the ORR/OER processes in the Cu ion contained electrolyte. To conclude, the Cu⁺/Cu²⁺ redox mediation effect facilitates the reversible decomposition of Li₂O₂ through the Cu⁺/Cu²⁺ redox dominated charge potential. Not only the energy efficiency has been improved, but also the high overpotential induced parasitic reactions (electrode degradation and electrolyte decomposition) are well suppressed.

The cycling performances of the Li-O₂ cells with Cu ion RM are finally investigated. As a soluble additive, the shuttling of RMs towards anode side would undoubtedly corrode the Li metal anode, which inflames the long term cycling test. In our case, the Cu ion in the electrolyte will definitely react with the bare Li anode, giving Cu deposited onto the anode (Fig. S8). To protect the Li anode from the Cu ion shuttling, a composite protection layer (CPL) is introduced onto the Li metal surface.^[30-32] Under the protection of CPL, the direct contact and Li metal corrosion have been inhibited, which can be proved by the XRD results (Fig. S8). This could also be confirmed through the cycling test at a low current density of $200 \text{ mA}\cdot\text{g}^{-1}$ (Fig. S9). Compared with the gradually increasing charge overpotential due to the failure

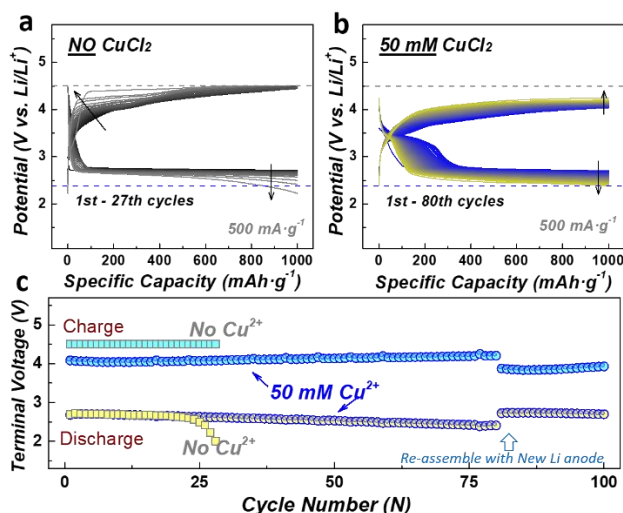


Fig. 4 Voltage profiles of Li-O₂ cells a) without and b) with Cu ion RM and a CPL protected Li anode. c) Terminal voltages versus cycles of Li-O₂ cells without and with Cu ion RM.

of Cu⁺/Cu²⁺ redox reacted with the bare Li anode, the Li-O₂ cell with the CPL covered Li anode exhibits stable electrochemical

curves with low charge potential. Fig. 4 displays the cycling performances of the corresponding Li-O₂ batteries at a current density of 500 mA·g⁻¹. Both batteries are equipped with a CPL covered Li metal anode. Assembled with bare electrolyte, the Li-O₂ cell exhibits large round-trip potential gaps and quickly fails after only 27 cycles. Once introduced with 50 mM Cu ion additive, the overpotential is apparently controlled, and the cycling stability is largely improved. Note that we still observe the gradually increasing overpotential for the Cu ion contained Li-O₂ cell, which is considered resulting from the increasing resistance at the anode side, owing to the corrosion of the Li anode. After reassembled the cycled KB cathode with a new Li metal covered with CPL, the potential gap recovers to the pristine state, indicating the stability of the carbon based cathode cycled with Cu ion redox couples. The influence of Cu ion concentration on the cycling performance is further discussed (Fig. S10). A trade-off relationship between the overpotential retention and anode stability is revealed. While high Cu ion concentration leads to lower overpotential, the stability of the Li metal anode is also affected. A more stable and durable protective layer is expected for the Li metal anode, which is the key issue for the practical application of mobile catalyst strategy for Li-O₂ batteries.

Conclusions

In conclusion, having widely realized its inherent defects, the development of Li-O₂ battery has gradually entered a post-solid-catalysis age. The rational and effective application of mobile catalyst to achieve the solution-mediated cell cycling has become a major development trend. Herein, we introduce an inorganic metal ion, Cu ion, as a multi-functional RM for Li-O₂ battery in several aspects: (1) As a RM_R, Cu⁺/Cu redox couple

helps exhibit a largely enhanced capacity of ~14700 mAh·g⁻¹ (~5.5 mAh·cm⁻²). (2) As a RM_E, Cu⁺/Cu²⁺ redox couple effectively lowers the charge potential to 3.5 V vs. Li⁺/Li, achieving high energy efficiency. (3) By restraining the superoxo-related parasitic reaction, the system stability and reversibility are enhanced. Not limited within the family of organic candidates, the original employment of Cu ion as a multi-functional additive opens up the new gate for the design of functional RMs, bringing in more potential candidates.

Conflicts of interest

There are no conflicts to declare.

Acknowledgements

This work was partially supported by the National Key Research and Development Program of China (2016YFB0100203), National Natural Science Foundation of China (21673116, 21633003), Natural Science Foundation of Jiangsu Province of China (BK20160068). The financial support by SPRING-ALCA from the Japan Science and Technology Agency (JST) is acknowledged. H.D. and Z.C. are grateful for financial support of the CSC (China Scholarship Council).

Notes and references

1. A. C. Luntz and B. D. McCloskey, *Chemical reviews*, 2014, **114**, 11721-11750.
2. M. Asadi, B. Sayahpour, P. Abbasi, A. T. Ngo, K. Karis, J. R. Jokisaari, C. Liu, B. Narayanan, M. Gerard, P. Yasaei, X. Hu, A. Mukherjee, K. C. Lau, R. S. Assary, F. Khalili-Araghi, R. F. Klie, L. A. Curtiss and A. Salehi-Khojin, *Nature*, 2018, **555**, 502-506.
3. M. M. Ottakam Thotiyl, S. A. Freunberger, Z. Peng and P. G. Bruce, *Journal of the American Chemical Society*, 2013, **135**, 494-500.
4. N. Feng, P. He and H. Zhou, *Advanced Energy Materials*, 2016, **6**, 1502303.
5. D. Aurbach, B. D. McCloskey, L. F. Nazar and P. G. Bruce, *Nature Energy*, 2016, **1**.
6. V. Viswanathan, K. S. Thygesen, J. S. Hummelshoj, J. K. Nørskov, G. Girishkumar, B. D. McCloskey and A. C. Luntz, *The Journal of chemical physics*, 2011, **135**, 214704.
7. J. Wang, Y. Zhang, L. Guo, E. Wang and Z. Peng, *Angewandte Chemie*, 2016, **55**, 5201-5205.
8. Z. Jian, P. Liu, F. Li, P. He, X. Guo, M. Chen and H. Zhou, *Angewandte Chemie*, 2014, **53**, 442-446.
9. Z. Li, S. Ganapathy, Y. Xu, Q. Zhu, W. Chen, I. Kochetkov, C. George, L. F. Nazar and M. Wagemaker, *Advanced Energy Materials*, 2018, **8**, 1703513.
10. X. Luo, L. Ge, L. Ma, A. J. Kropf, J. Wen, X. Zuo, Y. Ren, T. Wu, J. Lu and K. Amine, *Advanced Energy Materials*, 2018, **8**, 1703230.
11. J. B. Park, S. H. Lee, H. G. Jung, D. Aurbach and Y. K. Sun, *Advanced materials*, 2018, **30**.
12. B. D. McCloskey and D. Addison, *ACS Catalysis*, 2016, **7**, 772-778.
13. X. Gao, Y. Chen, L. Johnson and P. G. Bruce, *Nature materials*, 2016, **15**, 882-888.
14. Y. Zhang, L. Wang, X. Zhang, L. Guo, Y. Wang and Z. Peng, *Advanced materials*, 2018, **30**.

15. Y. Ko, H. Park, J. Kim, H.-D. Lim, B. Lee, G. Kwon, S. Lee, Y. Bae, S. K. Park and K. Kang, *Advanced Functional Materials*, 2019, **29**, 1805623.
16. B. J. Bergner, A. Schurmann, K. Peppler, A. Garsuch and J. Janek, *Journal of the American Chemical Society*, 2014, **136**, 15054-15064.
17. N. Feng, X. Mu, X. Zhang, P. He and H. Zhou, *ACS applied materials & interfaces*, 2017, **9**, 3733-3739.
18. Y. Chen, S. A. Freunberger, Z. Peng, O. Fontaine and P. G. Bruce, *Nature chemistry*, 2013, **5**, 489-494.
19. X. Gao, Y. Chen, L. R. Johnson, Z. P. Jovanov and P. G. Bruce, *Nature Energy*, 2017, **2**, 17118.
20. Y. Qiao, Y. He, S. Wu, K. Jiang, X. Li, S. Guo, P. He and H. Zhou, *ACS Energy Letters*, 2018, **3**, 463-468.
21. H. Deng, Y. Qiao, S. Wu, F. Qiu, N. Zhang, P. He and H. Zhou, *ACS applied materials & interfaces*, 2019, **11**, 4908-4914.
22. J. Zhang, B. Sun, Y. Zhao, A. Tkacheva, Z. Liu, K. Yan, X. Guo, A. M. McDonagh, D. Shanmukaraj, C. Wang, T. Rojo, M. Armand, Z. Peng and G. Wang, *Nature communications*, 2019, **10**, 602.
23. W. H. Ryu, F. S. Gittleson, J. M. Thomsen, J. Li, M. J. Schwab, G. W. Brudvig and A. D. Taylor, *Nature communications*, 2016, **7**, 12925.
24. D. Sun, Y. Shen, W. Zhang, L. Yu, Z. Yi, W. Yin, D. Wang, Y. Huang, J. Wang, D. Wang and J. B. Goodenough, *Journal of the American Chemical Society*, 2014, **136**, 8941-8946.
25. S. Matsuda, Y. Kubo, K. Uosaki, K. Hashimoto and S. Nakanishi, *The Journal of Physical Chemistry C*, 2016, **120**, 13360-13365.
26. M. C. Biesinger, L. W. M. Lau, A. R. Gerson and R. S. C. Smart, *Applied Surface Science*, 2010, **257**, 887-898.
27. J. Zhang, B. Sun, Y. Zhao, K. Kretschmer and G. Wang, *Angewandte Chemie*, 2017, **56**, 8505-8509.
28. Y. Qiao, S. Wu, J. Yi, Y. Sun, S. Guo, S. Yang, P. He and H. Zhou, *Angewandte Chemie*, 2017, **56**, 4960-4964.
29. D. Zhai, H. H. Wang, K. C. Lau, J. Gao, P. C. Redfern, F. Kang, B. Li, E. Indacochea, U. Das, H. H. Sun, H. J. Sun, K. Amine and L. A. Curtiss, *The journal of physical chemistry letters*, 2014, **5**, 2705-2710.
30. D. J. Lee, H. Lee, J. Song, M.-H. Ryou, Y. M. Lee, H.-T. Kim and J.-K. Park, *Electrochemistry Communications*, 2014, **40**, 45-48.
31. D. J. Lee, H. Lee, Y. J. Kim, J. K. Park and H. T. Kim, *Advanced materials*, 2016, **28**, 857-863.
32. W.-J. Kwak, S.-J. Park, H.-G. Jung and Y.-K. Sun, *Advanced Energy Materials*, 2018, **8**, 1702258.